

This article was downloaded by:

On: 29 January 2011

Access details: *Access Details: Free Access*

Publisher *Taylor & Francis*

Informa Ltd Registered in England and Wales Registered Number: 1072954 Registered office: Mortimer House, 37-41 Mortimer Street, London W1T 3JH, UK



## Supramolecular Chemistry

Publication details, including instructions for authors and subscription information:

<http://www.informaworld.com/smpp/title~content=t713649759>

### Nanozymes: Functional Nanoparticle-based Catalysts

Lucia Pasquato<sup>a</sup>; Paolo Pengo<sup>a</sup>; Paolo Scrimin<sup>b</sup>

<sup>a</sup> Department of Chemical Sciences, University of Trieste, Trieste, Italy <sup>b</sup> Department of Chemical Sciences, University of Padova, Padova, Italy

**To cite this Article** Pasquato, Lucia , Pengo, Paolo and Scrimin, Paolo(2010) 'Nanozymes: Functional Nanoparticle-based Catalysts', *Supramolecular Chemistry*, 18: 1, 163 – 171

**To link to this Article:** DOI: 10.1080/10610270412331328817

**URL:** <http://dx.doi.org/10.1080/10610270412331328817>

PLEASE SCROLL DOWN FOR ARTICLE

Full terms and conditions of use: <http://www.informaworld.com/terms-and-conditions-of-access.pdf>

This article may be used for research, teaching and private study purposes. Any substantial or systematic reproduction, re-distribution, re-selling, loan or sub-licensing, systematic supply or distribution in any form to anyone is expressly forbidden.

The publisher does not give any warranty express or implied or make any representation that the contents will be complete or accurate or up to date. The accuracy of any instructions, formulae and drug doses should be independently verified with primary sources. The publisher shall not be liable for any loss, actions, claims, proceedings, demand or costs or damages whatsoever or howsoever caused arising directly or indirectly in connection with or arising out of the use of this material.

# Nanozymes: Functional Nanoparticle-based Catalysts

LUCIA PASQUATO<sup>a</sup>, PAOLO PENGO<sup>a</sup> and PAOLO SCRIMIN<sup>b,\*</sup>

<sup>a</sup>Department of Chemical Sciences, University of Trieste, Via L. Giorgieri, 1 34127, Trieste, Italy; <sup>b</sup>Department of Chemical Sciences, University of Padova, Via F. Marzolo, 1 35131, Padova, Italy

Received (in Austin, USA) 26 July 2004; Accepted 20 September 2004

This short review highlights recent results on the use of nanoclusters of gold protected by a monolayer of functional ligands in both molecular recognition and catalysis. Particular emphasis is given to the multivalent properties of these systems and, in the case of catalysis, to the cooperativity between functional groups present in the ligands of the monolayer. The outstanding catalytic efficiency of some of the functional nanoparticles synthesized led us to call them *nanozymes* by analogy with the activity of catalytic polymers (*synzymes*).

**Keywords:** Nanoparticles; Supramolecular aggregates; Multivalency; Cooperative catalysis; Nanozymes

## INTRODUCTION

Nanosize clusters of several metals can act as templates for the self-assembly of organic molecules. For instance, organic thiols passivate the surface of gold nanoclusters forming a monolayer on their surface (Fig. 1). This prevents the growth of the particles and alters their solubility properties according to the functional groups present on the protecting monolayer. Synthetic procedures are available for the synthesis of these monolayer protected gold nanoparticles (Au-MPC) in both apolar [1,2] and polar solvents [3–6]. These materials are characterized by the properties of the organic molecules that constitute the monolayer but also by the properties of the metal cluster core [7–10]. The latter largely depend on the size of the cluster (i.e. the number of atoms) and are not discussed in this article apart from the fact that when the size of the core is larger than *ca.* 2.5–3 nm, it presents a characteristic plasmon resonance band with a maximum at 510–530 nm. The molar absorptivity of this band is particularly high so that it has been used

in many applications for the detection of specific events affecting its position, its intensity, or both [11]. In this review we focus on the protecting monolayer and mostly consider the gold core as a template for the (self)assembly of the monomers that constitute the monolayer components. Although the gold core can interact with different groups (amines, phosphines, thiols, etc.), thiols provide the energetically stronger interaction and are the most commonly used functional groups for gold nanoparticle functionalization.

## MOLECULAR RECOGNITION

The introduction in the thiols forming the monolayer of appropriate functional groups (ligand units) provides an entry to multivalent systems [12]. Under appropriate conditions and through the synergic action of the ligands, enhanced binding of substrates may be observed. This strategy has been exploited for the preparation of highly effective nanoparticles for the selective recognition of organic molecules with interesting applications in sensing. Two very different examples are presented here to illustrate this point. The first is in connection with the recognition of DNA and polynucleotides in general, while the second is concerned with the recognition of cell surfaces.

Thus by conjugating the ability of mercapto-alkaneoligonucleotide-modified gold nanoparticles to reciprocally interact in the presence of a complementary polynucleotide sequence with the change of color of the solution due to the formation of aggregates, Letsinger and Mirkin [13] were able to obtain a selective colorimetric detection system for

\*Corresponding author. E-mail: paolo.scrimin@unipd.it

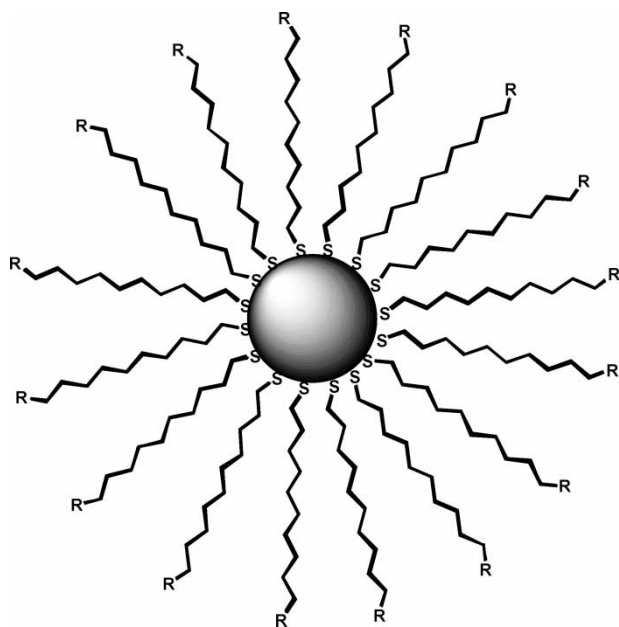


FIGURE 1 A monolayer-protected gold nanoparticle (Au-MPC). In this case the protecting monolayer comprises an alkanethiol.

polynucleotides. They chose  $\sim 13$  nm diameter gold particles that show a sharp plasmon absorption band with a wavelength maximum at 520 nm (their solution is red) for the functionalization with a thiol-terminated oligonucleotide. When the interparticle distance of the aggregates formed in the presence of the complementary polynucleotide is less than the average particle diameter, the plasmon absorption band shifts to a longer wavelength and the color of the solution becomes blue. Hence, without using radioactive groups or organic substituents, the gold nanoparticles become the reporter groups. The extended network of nanoparticles formed upon hybridization (Fig. 2) and resulting from the presence of several thiol-functionalized oligonucleotides on each nanoparticle is at the basis of the sensing system.

With a different approach polyvalence has been exploited for the electrostatic binding of DNA via its negatively charged phosphate groups, with positively charged quaternary ammonium ions introduced on the surface of the MPC [14]. It has been established that these gold nanoparticles, protected by a mixed monolayer composed of octanethiol and 11-trimethylammonium undecanethiol units, bind DNA in a stoichiometric, nonaggregated fashion. Moreover, these MPCs display not only the DNA-binding ability common to multiply charged systems, such as polymers, dendrimers or small molecules, but also the capability of inhibiting a transcription enzyme, T7 RNA polymerase, from producing RNA products.

Linking carbohydrates to gold nanoparticles is a method for tailoring highly polyvalent water-soluble

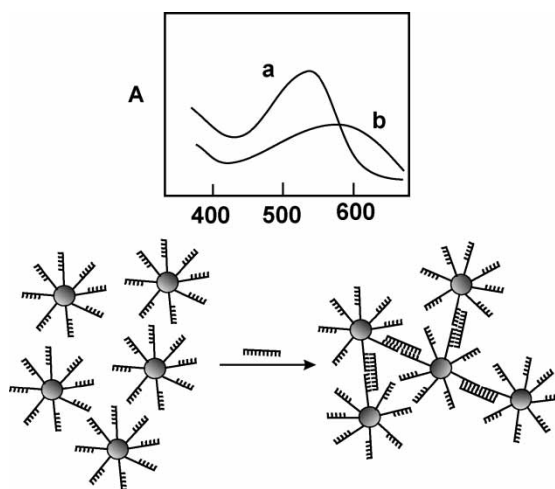


FIGURE 2 Oligonucleotide-functionalized gold nanoparticles aggregate upon hybridization with complementary DNA. The process is associated with a change in the absorption wavelength of the surface plasmon band that is centered at  $\sim 520$  nm before aggregation (a) and moves close to  $\sim 600$  nm after aggregation (b).

carbohydrate surfaces with globular shapes. This approach opens the way to the preparation of glyconanoparticles with a variety of carbohydrate ligands on their surface and with different ligand densities. Such systems are suitable models for the investigation of the effects of carbohydrate clustering and orientation on the interactions with specific receptors. The need for polyvalent systems stems from the fact that the monovalent carbohydrate-protein or carbohydrate-carbohydrate interactions are generally characterized by very low affinity. In natural systems, the presentation of multiple ligands to individual receptors can compensate for the low affinity because the polyvalent interactions between multiligands and their receptors can be collectively much stronger than the corresponding monovalent interactions [12].

The synthesis of water-soluble gold glyconanoparticles was first reported by Penadés and coworkers [15]. The strategy used was to self-assemble the target thiol- or disulfide-derivatized glycoconjugates on the gold nanoparticles using the procedure of Brust *et al.* [1]. Two biologically significant oligosaccharides, the disaccharide lactose ( $\text{Gal}\beta(1 \rightarrow 4)\text{Glc}\beta 1\text{-OR}$ ) and the trisaccharide  $\text{Le}^x$  ( $\text{Gal}\beta(1 \rightarrow 4)[\text{Fuc}\alpha(1 \rightarrow 3)]\text{GlcNAc}\beta 1\text{-OR}$ ), were prepared to functionalize gold nanoparticles (Fig. 3).

The glyconanoparticles were used as 3D models to mimic GSL clustering at the cell surface and to investigate carbohydrate-carbohydrate interactions in solution. Divalent cations such as  $\text{Ca}^{2+}$  mediate the association process of the glyconanoparticles, which is reversible as shown by the addition of EDTA.

All the above examples stress the importance of multiple recognition events in attaining strong

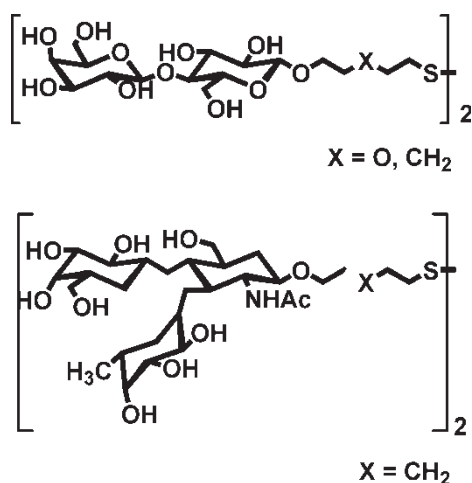


FIGURE 3 Structure of the glycoside ligands used in nanoparticle protection.

(and selective) binding. However, in no case was the individual contribution of each monomeric ligand to the overall binding process estimated. We have recently reported a compelling example of multivalent recognition based on functional gold nanoparticles where the single contribution of each binding event could be dissected [16]. *N*-Methylimidazole-functionalized gold nanoparticles have been used to bind mono-, bis- and tris-Zn-porphyrins (Fig. 4). As the number of porphyrins increased, the relative gain in binding constant ( $\beta$ ) and effective molarity (EM) for intracomplex binding became lower. By extrapolating this trend we can speculate that, by increasing the number of porphyrins in the array, the binding constant will reach a limiting value with no further improvement. This could be

the result of the poor fitting of the porphyrin array to the curved surface of the MPCs or to the accumulation of adverse interactions with the surface (steric interactions between porphyrins and monolayer). Nevertheless, it should be noted that the values of  $\beta$  and EM observed for the tris-porphyrin were slightly higher than those reported previously using a tripodal methylimidazole derivative (see Fig. 4) with a structure complementary to that of the tris-Zn-porphyrin used [17]. This indicates that the cooperative binding of the methylimidazoles on the nanoparticles to the tris-porphyrin is as good as, or better than, that of the tripodal ligand.

## CATALYSIS

It occurred to us that multivalency, at the basis of the amplification of the binding events with functional nanoparticles, could be exploited for the preparation of catalytic systems where a cluster of functional groups may lead to a catalytic activity that is not just the summation of the individual contributions. This has been a "holy grail" for everyone using self-assembled aggregates for catalysis. In a review written more than 10 years ago [18], Fred Menger wrote, with reference to colloid aggregates: "groups of molecules, properly assembled, can obviously accomplish much more than an equal number of molecules functioning separately." In the case of micelles or vesicles this statement led to some controversy as much evidence suggested that the large rate accelerations observed with these systems were mostly related to concentration effects rather than to real cooperativity between the constituents

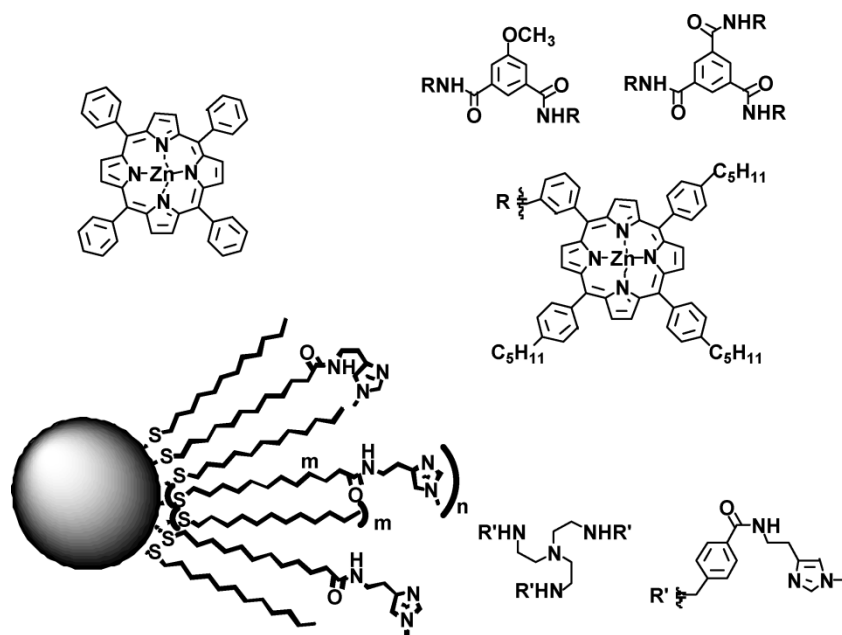


FIGURE 4 Imidazole-functionalized Au-MPC used for polyvalent binding of multiporphyrin systems.

[19,20]. The reason for this behavior is mostly entropic as in these aggregates the constituent monomers enjoy a large amount of motional freedom. However, this is not the case for the functional thiols covering the surface of gold nanoparticles as their mobility is rather limited, being anchored on the surface of the gold nanocluster. A case in point is provided by our recent results concerning the determination of the polarity of the monolayer of hydrocarbon/polyether-covered gold nanoparticles. By using EPR spectroscopy we have determined the partition isotherms and exchange rates of a radical probe between the aqueous solution and the monolayer of these water-soluble Au-MPCs [21]. Contrary to micelles, where it is impossible to know precisely how the monomers aggregate due to the disorder of the system, the monolayer showed well-defined regions due to the specific orientation of the constituent thiols. This allowed us to identify with confidence the locations of the amphiphilic probes in the monolayer at the boundary between the hydrocarbon and polyether regions, although partition isotherms and rate of exchange were governed by the hydrophobic portions of the probes. The hypothesis is thus well founded that the protecting monolayer of Au-MPCs may act as a unique environment with well-defined subregions and, most importantly, with controlled relative positions of the functional groups present in the gold-passivating thiols [22].

Our first system was the very simple *N*-methylimidazole-functionalized Au-MPCs shown in Fig. 4 [23]. Imidazoles of histidines are key functional groups present in the catalytic site of many proteolytic and esterolytic enzymes. They typically work cooperatively via base/nucleophilic- and acid-catalyzed mechanisms and are, accordingly, excellent candidates for testing cooperativity in a catalyst for the cleavage of carboxylate esters. The functional nanoparticles were prepared by exchange reaction by codissolving in methylene chloride/methanol (1:1) dodecanethiol-protected gold nanoparticles (Au-MPC-C12) and the functional thiol under conditions with an entering to exiting ligand ratio of 1:1.5. The resulting material was purified by exclusion chromatography. Cleavage of 2,4-dinitrophenyl acetate (DNPA), as a model ester, was studied in a methanol–water (6:4) solution, in which the new MPCs are fully soluble, in the pH range 4.5–7.2. The reactions were monitored by UV–vis following the formation of 2,4-dinitrophenolate at 400 nm and 25°C. For comparison purposes acetyl-*N*-methylhistamine was also used as a reference monomeric catalyst. The dependence of the second-order rate constant,  $k_2$ , on pH for the imidazole-functionalized Au-MPC and the monomeric catalyst is shown in Fig. 5, where the remarkable rate acceleration exerted by the nanoparticles relative to the monomeric catalyst can be readily appreciated. Although the  $pK_a$  of *N*-methylimidazole in the nanoparticles could not be determined because of their insolubility at

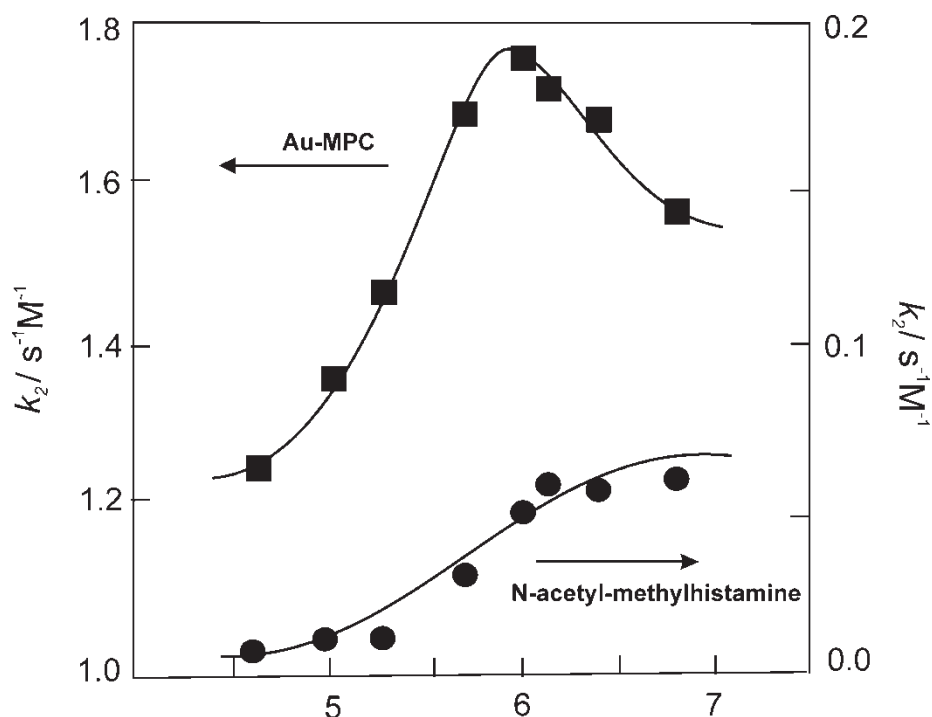


FIGURE 5 Dependence of second-order rate constants,  $k_2$ , on pH for the cleavage of DNPA catalyzed by the imidazole-functionalized nanoparticles shown in Fig. 4 (upper curve) and by *N*-methylacetyl histamine (lower curve).



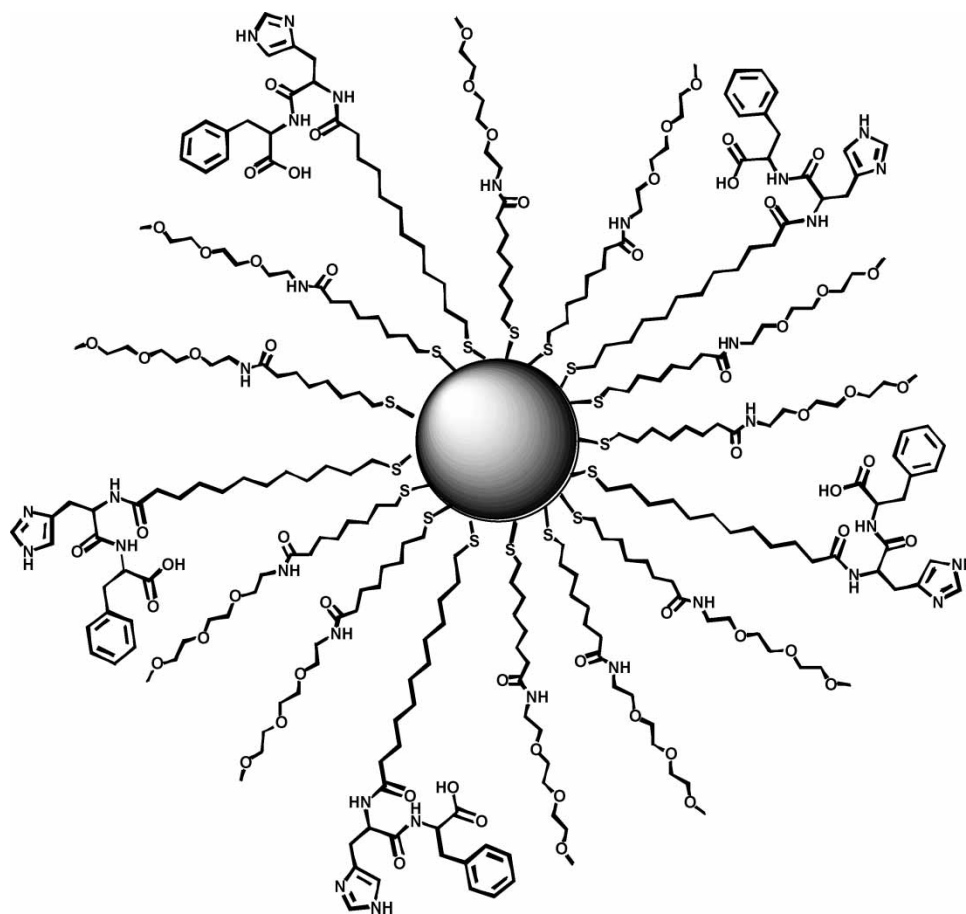


FIGURE 6 HisPhe dipeptide-functionalized nanoparticles used for the cleavage of DNPB.

the high concentration required for the potentiometric titration, it is likely to be similar to the value found for the monomer (6.2) in the solvent mixture used for the kinetic experiments. The low dependence of  $k_2$  on pH in the pH range 5–7, with a small maximum in the proximity of the  $pK_a$ , supports cooperativity between two methylimidazoles in the DNPA cleavage by the nanocluster (general acid/general base or nucleophilic catalysis). The solid curves of Fig. 5 represent the computer-generated best fitting of the experimental points assuming a cooperative process (Au-MPC) and nucleophilic catalysis (monomeric system). A fair comparison between the two systems can be made at the pH values of the maxima of the two curves (pH 7.2 for the monomer and 6.1 for the nanocluster). Under these conditions the nanocluster-catalyzed process is *ca.* 30 times faster than that observed using the monomer.

Further elaborating on the structure of the catalytic site we prepared a thiol-functionalized dipeptide by *N*-acylation of HisPhe. We speculated that, in this system, the free carboxylate/carboxylic acid of phenyl alanine could add a further function for catalysis providing, as in the case of imidazole, base/nucleophilic and/or acid catalytic

contributions. The nanoparticles were prepared by exchange reaction starting from our polyether-functionalized water-soluble nanoparticles, thus affording the new Au-MPCs shown in Fig. 6 [24]. This new system could be studied in an aqueous solution where hydrophobic interactions can be exploited for the recognition of a substrate. Indeed these nanoparticles bind the lipophilic *p*-nitrophenyl ester of *Z*-protected *L*-leucine with a binding constant,  $K_b$ , of  $2 \times 10^4 \text{ M}^{-1}$ . Contrary to the previous system, the dipeptide-based catalyst did not show any evidence of cooperativity between two imidazoles but, rather, the nucleophilic contribution of both an imidazole and a carboxylate in the cleavage of 2,4-dinitrophenylbutanoate (DNPB). Preliminary experiments indicate little (if any) dependence from the functional/nonfunctional thiol ratio in the monolayer. This may be due to intrathiol cooperativity between carboxylate and imidazole or to sorting of the functional thiol within the monolayer. This is an important point that is very difficult to address with appropriate experiments. In any case the carboxylate contribution provided a rate acceleration with respect to the monomer larger than two orders of magnitude. Because of this, these functional Au-MPCs may be considered as models of

an aspartic esterase and, like the real enzyme, show maximum efficiency below pH 5.

The ultimate goal we had in mind was the mimicry of an esterolytic enzyme not just by introducing minimal functional groups at the periphery of the nanoparticles but also by providing the appropriate environment (including chirality) as in the catalytic site of a protein. What we were pursuing was the self-assembly of a synthetic protein by grafting on the surface of a gold nanoparticle short but conformationally constrained peptides. Very naively we made our first approach by using the rather lipophilic (although highly structured [25] in a helical conformation) peptide shown in Fig. 7 [26], assuming that the imidazole would be sufficient for water solubilization. Although the exchange reaction with Au-MPC-C12 was successful, the resulting system proved to be scarcely soluble not only in an aqueous solution but also in a variety of solvents of different polarity. The likely explanation is that the packing of the peptide in the monolayer is too tight,

resulting in an extended network of intramonolayer hydrogen bonds preventing solubilization.

We learned two lessons: the first was that water-soluble nanoparticles had to be used for the exchange reaction; and the second was that the exchange of the thiols had to be limited to avoid overcrowding in the monolayer. By applying these rules of thumb we succeeded in preparing nanoparticles covered by a monolayer comprising the dodecapeptide shown in Fig. 8. The sequence terminates with the free carboxylate of arginine and presents several functional groups potentially active for the catalysis of the cleavage of a carboxylate ester: one histidine, flanked by hydrophobic amino acids, one lysine and one tyrosine. These nanoparticles were fully soluble in water over a wide pH range and showed remarkable activity in the cleavage of DNPB. However, while the dipeptide-functionalized Au-MPCs were particularly efficient at low pH, these new nanoparticles proved particularly effective at pH higher than 8: a clear indication that they

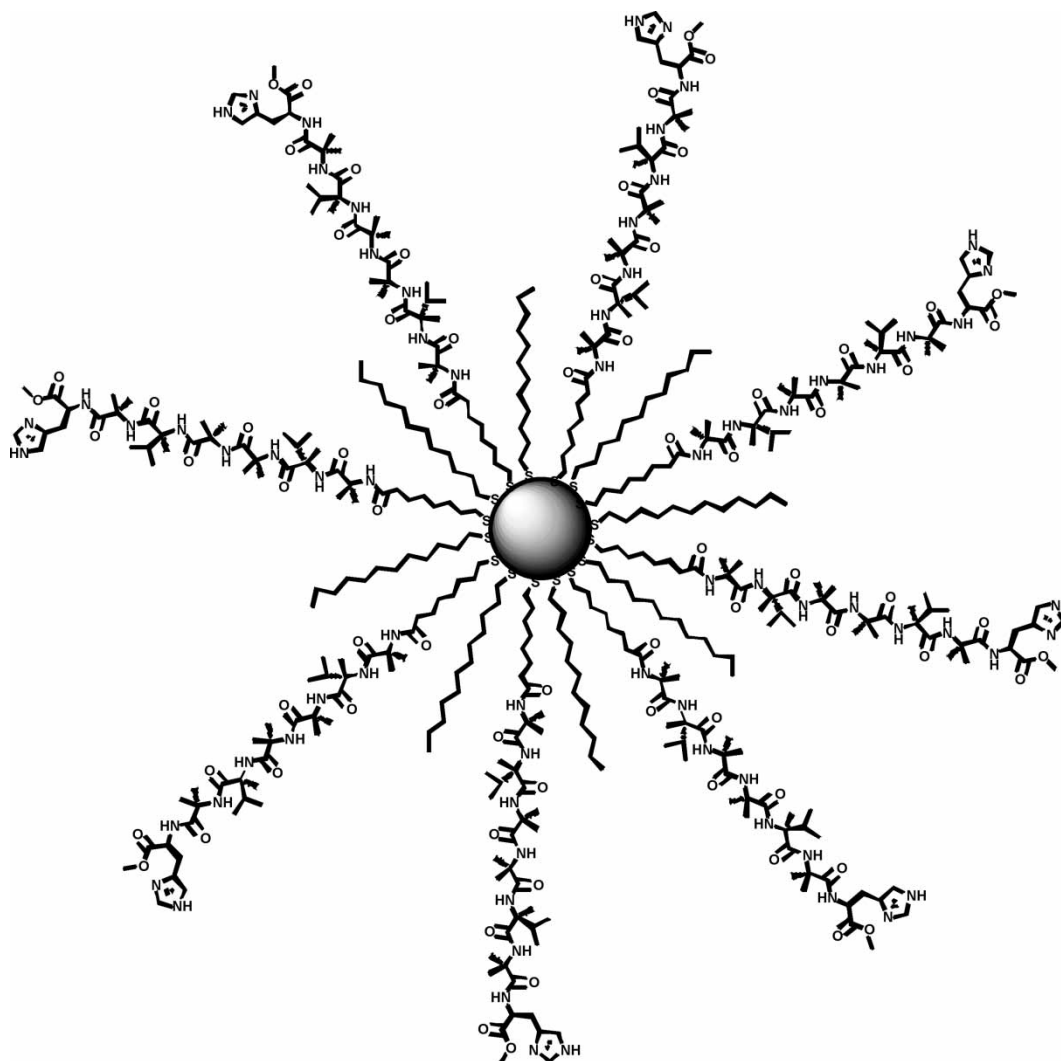


FIGURE 7 Heptapeptide-functionalized Au-MPCs. In this rendition the peptide is shown in its extended conformation and hence appears as extending well above the hydrocarbon monolayer. In reality, because of its helical conformation it is much shorter (about 15 Å).

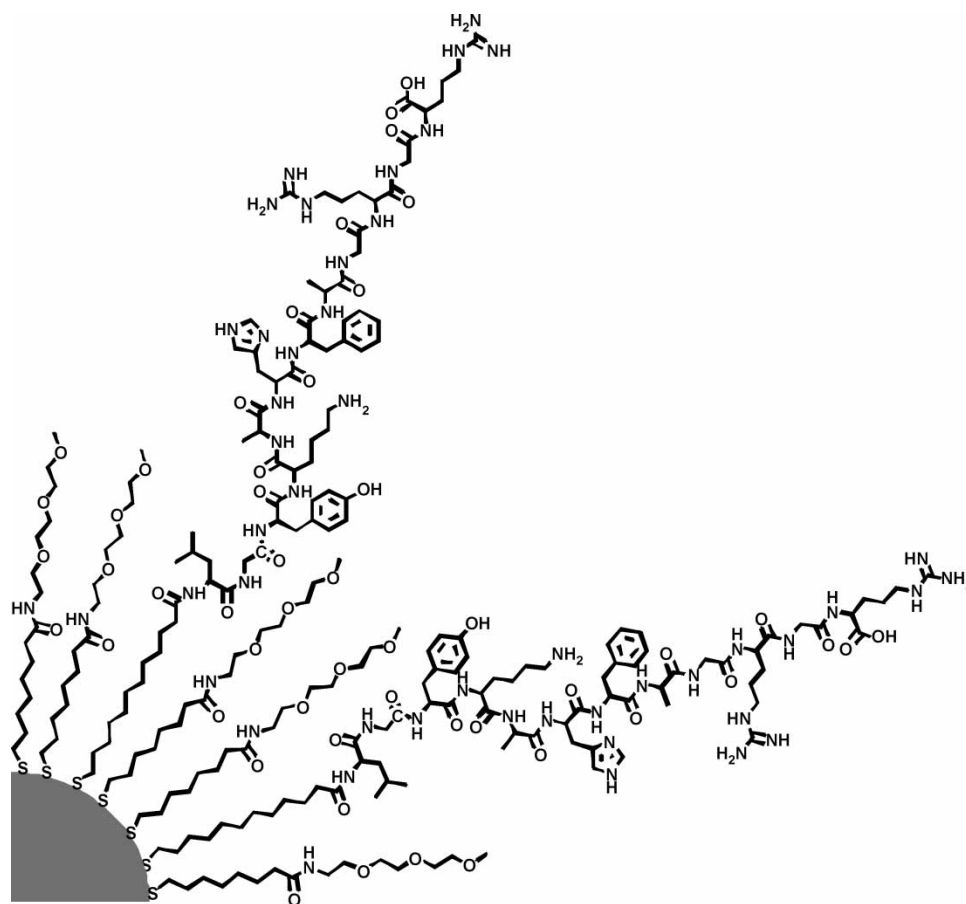


FIGURE 8 Pie slice representation of the dodecapeptide-functionalized Au-MPCs. As in the case of the peptide of Fig. 7, the extended conformation of the peptide shown here is not completely accurate as in reality it is more compact.

were working preferentially with a base-catalyzed or nucleophilic mechanism involving high  $pK_a$  species. The complete analysis of the system is still under way but we know already that the rate acceleration at pH 10 is about two order of magnitude larger than that determined with the dipeptide-functionalized nanoparticles while at the low pH regime the acceleration is similar.

All the above results point to a single direction: the functional groups present in the protecting monolayer of Au-MPCs show unique catalytic properties deriving from their confinement in space, which in turn results in a cooperative action. Thus, what was controversial (cooperativity) with classical aggregation colloids like micelles and vesicles appears to be the rule with the nanoparticles!

Perhaps the most striking example of cooperativity is that shown by the ligand-functionalized Au-MPCs we have very recently reported (Fig. 9) [27]. These nanoclusters were used, as  $Zn^{II}$  complexes, as catalysts for the cleavage of phosphate esters in the mimicry of an RNase.

Most of these enzymes require for their activity at least two metal ions that act cooperatively in the process [28,29]. A thorough analysis of the system was carried out by using 2-hydroxypropyl

*p*-nitrophenyl phosphate (HPNP) as the substrate, an activated phosphate diester frequently used as a model of RNA. With HPNP the release of *p*-nitrophenol (or *p*-nitrophenolate, depending on the pH) is accompanied by the formation of a cyclic phosphate [30] and can be easily followed spectrophotometrically. Figure 10 reports the reactivity profile obtained by progressively adding  $Zn^{II}$  ions to a solution of these nanoparticles up to the saturation of the metal ion binding subunits. This kinetic analysis reveals that: (a) the most active system is the one fully loaded with  $Zn^{II}$  ions; and (b) the sigmoidal profile of the curve supports cooperativity between the metal centers as the catalytic efficiency becomes much higher after the first 30% of  $Zn^{II}$  ions is added. The real catalytic nature of the process was assessed by carrying out experiments with excess substrate. No formation of an intermediate was detected and well-behaved first-order kinetics were observed up to the complete cleavage of all substrate present. By varying the initial substrate concentration, a kinetic profile towards saturation was observed. These kinetics allowed the determination of the apparent Michaelis-Menten parameters  $K_M$  and  $k_{cat}$  0.93 mM and  $4.2 \times 10^{-3} s^{-1}$ , respectively. The formal second-order rate constant for HPNP cleavage ( $k_{cat}/K_M$ ) by  $Zn^{II}$ -saturated



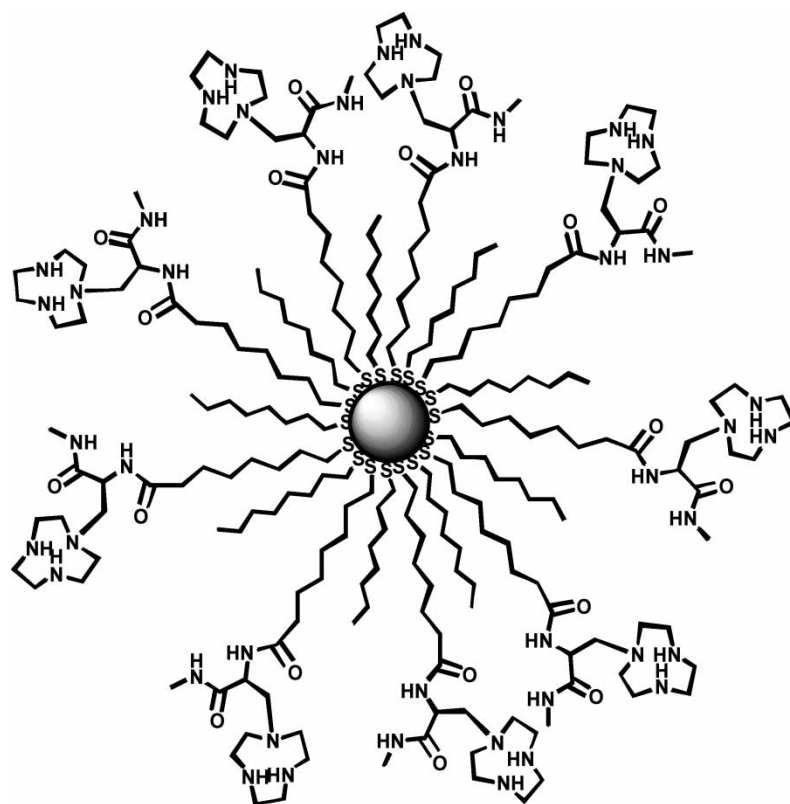


FIGURE 9 Azacrown-functionalized Au-MPCs. Their  $\text{Zn}^{\text{II}}$  complex is a model of an RNase.

nanocluster has been determined to be  $4.4 \text{ s}^{-1} \text{ M}^{-1}$ , which is more than 600 times higher than that measured under identical conditions for the mononuclear catalyst corresponding to the "active unit" on the surface of the Au-MPCs. The  $k_{\text{cat}}$

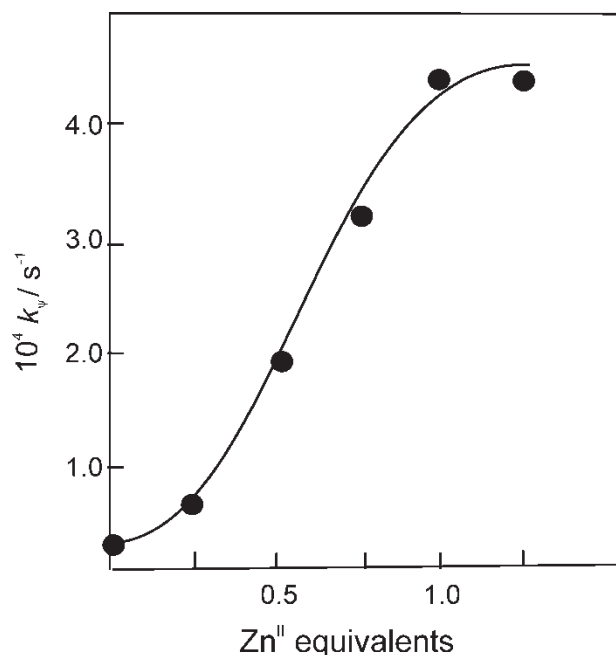


FIGURE 10 Reactivity profile in the cleavage of HPNP for the functional Au-MPCs of Fig. 9 by progressive addition of  $\text{Zn}^{\text{II}}$  ions.

of  $\text{Zn}^{\text{II}}$ -Au-MPCs was comparable to that of the best multinuclear  $\text{Zn}^{\text{II}}$  catalysts for HPNP cleavage reported so far [31] based on calyx[10]arene functionalized with two or three 2,6-diaminomethylpyridine units and thus able to bind up to three  $\text{Zn}^{\text{II}}$  ions. The kinetic profile indicated that the role of the metal ions was that of stabilizing the complexed substrate towards the transition state, where a further negative charge develops, and in facilitating deprotonation of the nucleophilic species. With such an outstanding catalyst in hand we turned to more appealing substrates such as RNA dinucleotides (3',5'-NpN), namely ApA, CpC and UpU. Their uncatalyzed cleavage is extremely slow with rate constants (pH 7) ranging from  $9.8 \times 10^{-9} \text{ s}^{-1}$  (UpU) [32] to  $1.7 \times 10^{-9} \text{ s}^{-1}$  (ApA) [33], that is about two orders of magnitude less reactive than HPNP. As in the case of HPNP, the process is an intramolecular transesterification, in this case by the hydroxyl group at the 2'-position of the ribose. At pH 7.5 (5 mM HEPES buffer) and 40°C,  $\text{Zn}^{\text{II}}$ -Au-MPCs cleaved ApA, CpC and UpU with second-order rate constants of  $3.0 \times 10^{-4}$ ,  $3.6 \times 10^{-4}$  and  $1.2 \times 10^{-2} \text{ s}^{-1} \text{ M}^{-1}$ , respectively. Thus catalyst  $\text{Zn}^{\text{II}}$ -Au-MPCs was also fairly active in the cleavage of RNA dinucleotides. Very interestingly, it showed a remarkable selectivity in the cleavage of UpU, probably due to a preferential binding of this substrate on the functional surface of the nanoparticles.

## CONCLUSIONS

The passivation of gold nanoparticles with a monolayer of functional thiol is a straightforward way to synthesize new supramolecular assemblies that may act cooperatively in the recognition of substrates and in performing catalytic processes. These Au-MPCs are polyvalent systems, where the confinement of the monomers on the monolayer alters their properties, with outstanding results in binding and, more importantly, in catalysis. This behavior led us to call them *nanozymes* [27] by analogy with the activity of catalytic polymers (synzymes). We have shown here a selection of these systems and anticipate that by changing the nature of the functional units present on the gold-protecting monolayer, we can further expand the repertoire of powerful, self-assembled catalysts (nanozymes) obtainable, of which those reported here constitute just prototypes.

## References

- [1] Brust, M.; Walker, M.; Bethell, D.; Schiffrin, D.; Whyman, R. *J. Chem. Soc. Chem. Commun.* **1994**, 801.
- [2] Hostetler, M. J.; Wingate, J. E.; Zhong, C.-J.; Harris, J. E.; Vachet, R. W.; Clark, M. R.; Londono, J. D.; Green, S. J.; Stokes, J. J.; Wignall, G. D.; Glish, G. L.; Porter, M. D.; Evans, N. D.; Murray, R. W. *J. Am. Chem. Soc.* **1998**, *120*, 1906.
- [3] Pengo, P.; Polizzi, S.; Battagliarin, M.; Pasquato, L.; Scrimin, P. *J. Mater. Chem.* **2003**, *13*, 2471.
- [4] Brust, M.; Bethell, D.; Schiffrin, D. J.; Kiely, C. *J. Chem. Soc., Chem. Commun.* **1995**, 1655.
- [5] Zheng, M.; Davidson, F.; Huang, X. *J. Am. Chem. Soc.* **2003**, *125*, 7790.
- [6] Foos, E. E.; Snow, A. W.; Twigg, M. E.; Ancona, M. G. *Chem. Mater.* **2002**, *14*, 2401.
- [7] Daniel, M.-C.; Astruc, D. *Chem. Rev.* **2004**, *104*, 293.
- [8] Templeton, A. C.; Wuelfing, W. P.; Murray, R. W. *Acc. Chem. Res.* **2000**, *33*, 27.
- [9] Badia, A.; Lennox, R. B.; Reven, L. *Acc. Chem. Res.* **2000**, *33*, 475.
- [10] Shenhar, R.; Rotello, V. M. *Acc. Chem. Res.* **2003**, *36*, 549.
- [11] Pasquato, L.; Pengo, P.; Scrimin, P. In *Nanoparticles. Building Blocks for Nanotechnology*; Rotello, V., Ed.; Kluwer Academic/Plenum Publishers: New York, 2003; pp 251–282.
- [12] Mammen, M.; Choi, S.-K.; Whitesides, G. M. *Angew. Chem., Int. Ed. Engl.* **1998**, *37*, 2754.
- [13] Elghanian, R.; Storhoff, J. J.; Mucic, R. C.; Letsinger, R. L.; Mirkin, C. A. *Science* **1997**, *277*, 1078.
- [14] McIntosh, C. M.; Esposito, III, E. A.; Boal, A. K.; Simard, J. M.; Martin, C. T.; Rotello, V. M. *J. Am. Chem. Soc.* **2001**, *123*, 7626.
- [15] de la Fuente, J.; Barrientos, A. G.; Rojas, T. C.; Rojo, J.; Cañada, J.; Fernández, A.; Penadés, S. *Angew. Chem. Int. Ed. Engl.* **2001**, *40*, 2257.
- [16] Fantuzzi, G.; Pengo, P.; Gomilla, R.; Ballester, P.; Hunter, C. A.; Pasquato, L.; Scrimin, P. *Chem. Commun.* **2003**, 1004.
- [17] Felluga, F.; Tecilla, P.; Hillier, L.; Hunter, C. A.; Licini, G.; Scrimin, P. *Chem. Commun.* **2000**, 1087.
- [18] Menger, F. M. *Angew. Chem. Int. Ed. Engl.* **1991**, *30*, 1086.
- [19] Bunton, C. A.; Nome, F.; Quina, F. H.; Romsted, L. *Acc. Chem. Res.* **1991**, *24*, 357.
- [20] Scrimin, P.; Tecilla, P.; Tonellato, U.; Bunton, C. A. *Coll. Surf. (A)* **1998**, *144*, 71.
- [21] Lucarini, M.; Franchi, P.; Pedulli, G. F.; Pengo, P.; Scrimin, P.; Pasquato, L. *J. Am. Chem. Soc.* **2004**, *126*, 000.
- [22] For an example of vectorial dependence of kinetic processes within a monolayer see: Briggs, C.; Norsten, T. B.; Rotello, V. M. *Chem. Commun.* **2002**, 1890.
- [23] Pasquato, L.; Rancan, F.; Scrimin, P.; Mancin, F.; Frigeri, C. *Chem. Commun.* **2000**, 2253.
- [24] Pengo, P.; Pasquato, L.; Scrimin, P., submitted for publication.
- [25] Pengo, P.; Pasquato, L.; Moro, S.; Brigo, A.; Fogolari, F.; Broxterman, Q. B.; Kaptein, B.; Scrimin, P. *Angew. Chem. Int. Ed. Engl.* **2003**, *42*, 3388.
- [26] Pengo, P.; Broxterman, Q. B.; Kaptein, B.; Pasquato, L.; Scrimin, P. *Langmuir* **2003**, *19*, 2521.
- [27] Manea, F.; Bodar Houillon, F.; Pasquato, L.; Scrimin, P. *Angew. Chem. Int. Ed. Engl.* **2004**, *43*, 0000.
- [28] Sträter, N.; Lipscomb, W. N.; Klabunde, T.; Krebs, B. *Angew. Chem., Int. Ed. Engl.* **1996**, *35*, 2024.
- [29] Wilcox, D. E. *Chem. Rev.* **1996**, *96*, 2435.
- [30] Bonfà, L.; Gatos, M.; Mancin, F.; Tecilla, P.; Tonellato, U. *Inorg. Chem.* **2003**, *42*, 3943.
- [31] Molenveld, P.; Stikvoort, W. M. G.; Kooijman, H.; Spek, A. L.; Engbersen, J. F. J.; Reinhoudt, D. N. *J. Org. Chem.* **1999**, *64*, 3896.
- [32] Chapman, W. H., Jr.; Breslow, R. *J. Am. Chem. Soc.* **1995**, *117*, 5462.
- [33] Komiya, M.; Yoshinari, K. *J. Org. Chem.* **1997**, *62*, 2155.